Alignment effects in charge transfer and excitation for H^+ and He^{2+} collisions with H_2^+

D. J. Phalen,* M. S. Pindzola, and F. Robicheaux†
Department of Physics, Auburn University, Auburn, Alabama 36849-5311, USA
(Received 4 November 2004; published 19 August 2005)

The excitation and charge transfer cross sections are calculated for the collision of H^+ and He^{2+} with H_2^+ molecular ions. This is the simplest example of collisions between ions and molecules or molecular ions since it involves only one electron. The results in this paper emphasize effects due to the alignment of the axis of the H_2^+ molecular ion relative to the atomic ion velocity vector and due to the internuclear separation. The calculations show that the cross section versus the angle between the molecular ion axis and the ion velocity vector strongly depends on the ion velocity. Our results for He^{2+} collisions do not agree with the experiments and calculations of Reiser, Cocke, and Bräuning [Phys. Rev. A **67**, 062718 (2003)] but are in qualitative agreement with the calculations of Cheng and Esry.

DOI: 10.1103/PhysRevA.72.022720 PACS number(s): 34.70.+e, 34.50.Lf, 34.50.Gb

I. INTRODUCTION

The study of ion-atom collisions has a long history for both experimental and theoretical techniques. There has been much less effort for ion-molecule collisions. Computationally, the ion-molecule collisions are much more difficult than ion-atom collisions. This is partly due to the multicenter nature of the problem instead of the two centers for ion-atom collisions. Perhaps more importantly, the cross sections may depend on several other coordinates. Thus, there is a dramatic increase in the number of calculations needed to explore the physically relevant parameters. There is also the possibility that interference due to the extended size of the electron orbitals will cause the results to depend sensitively on the accuracy of the calculation. Finally, molecules have a larger number of low-lying excited states compared to similar atoms which may sensitively affect the outcome of collisions.

To see where some of the difficulties lie, we examine what is needed for ions scattering from a diatomic molecule that has no initial angular momentum about the internuclear axis. We simplify the picture further by assuming the ion may be treated as a classical particle traveling in a straight line and the nuclei in the molecule may be treated as fixed in space during the collision. In the comparable case for ion-atom collisions, one only needs to calculate the probability for a process as a function of the impact parameter. For the ion-molecule collision, the probability for a process needs to be calculated as a function of the impact parameter *in a plane* (i.e., two dimensions), as a function of the separation of the nuclei, and as a function of the angle between the ion's velocity and the internuclear axis. Thus, we have gone from one parameter to four; assuming we need 5–10 examples of each parameter for an adequate exploration of ion-molecule collision we find there are approximately 100–1000 times more trajectories that are needed for ion-molecule calculations than for a comparable ion-atom calculation.

The simplest ion-molecule system is when there is only one electron present. References [1,2] studied the collision of He^{2+} with the D_2^+ molecular ion. Reference [1] measured the total charge transfer cross section and compared the results to calculations using a model for the electronic orbital for the molecule. The model used a linear combination of atomic orbitals and the transition amplitudes are approximated as a linear superposition of the amplitudes for each atomic orbital [3]. The calculated and measured total charge transfer cross sections were in good agreement. Reference [2] measured the dependence of the total charge transfer cross section on the angle between the velocity of the atomic ion and the internuclear axis and compared the measurement to the results of a model calculation again based on Ref. [3]. Although the agreement was not as good, the general trends were the same: the cross section is much larger for perpendicular geometry than when the velocity is parallel to the internuclear axis. At velocity 0.4 a.u., the measurement gives a cross section 3–4 times larger at 90° than at 0° while the calculation gives a factor of 7–8. At velocity 0.5 a.u., the measurement gives a cross section 3–6 times larger at 90° compared to 1.5–2 for the calculation. Reference [4] presents calculations for total charge transfer for this system using both classical methods and a (2+1)-center close-coupling approximation. The total charge transfer cross section was 20–30 % lower than the previous measurement and calculation.

In this paper, we present the results of calculations for charge transfer from the H_2^+ molecular ion to He^{2+} ions and to H^+ ions. Because the protons of the molecular ion are fixed during the collision, our results apply equally well to D_2^+. The focus of this paper is the dependence of the cross section on the angle between the ion's velocity vector and the internuclear axis and the dependence on the internuclear separation. Our method of calculation consists of direct numerical solution of Schrödinger's equation on a grid of points; grid methods can be thought of as a basis set method with the number of basis functions equal to the number of grid points ($>10^7$ in our case) but with a momentum cutoff roughly equal to the inverse of the separation of grid points.

*Present address: Department of Physics and Astronomy, Rice University, Houston, Texas 77005.
†Electronic address: robicfj@auburn.edu

In contrast, basis set methods usually have many fewer basis functions and a much lower cutoff in momentum; in some cases, basis set methods can have an advantage when singularities in the wave function (e.g., cusps) are directly included in the basis set or can have an advantage in multielectron systems where the crudeness in the grid spacing prevents accurate solution. Thus for this one-electron problem, we expect the grid methods to give a more complete representation of the bound and continuum character of the electron's wave function. We compare our results to the previous calculations and measurements where possible. The present calculations were inspired by the results of Ref. [5]; our method is very similar to theirs, but our results should be better converged since we were able to use a finer grid.

Atomic units are used unless specifically stated otherwise.

II. COMPUTATIONAL METHOD

A. Classical nuclei approximations

In all of our calculations, we treated the ion as a classical particle that travels with a constant velocity vector and we treated the two protons in H_2^+ as stationary point charges. The ion is traveling at speeds greater than 0.4 a.u. resulting in a very small de Broglie wavelength (less than 1/120 a.u. in all calculations). Thus, it seems that approximating the ion as a classical particle should give accurate results. Also, the kinetic energy of the ion is at least 4 keV. Therefore, the trajectory of the ion will not be substantially deflected for impact parameters greater than 0.05 a.u.; this limit is much smaller than the impact parameters used in the calculation. The time required for the ion to travel a distance twice the size of the molecule is less than 10 a.u. The rotational and vibrational periods of H_2^+ are much longer than this time. Thus, the protons in H_2^+ can be treated as fixed in space during the collision. Because the protons in the molecule are fixed, our results apply equally well to D_2^+ for which there are measurements and we will refer to the molecular ion in either isotopic form.

B. Quantum electron

The only quantum particle in the calculation is the electron. We solve for the electron's wave function using a technique similar to that described in Ref. [6]. The wave function is represented by a Cartesian grid of points with equal spacing in all three directions. The kinetic energy operator acting on the wave function is approximated using a three-point difference in each direction:

$$(T\Psi)_{j,k,l} = -\frac{1}{2\Delta x^2}(\Psi_{j+1,k,l} + \Psi_{j-1,k,l} + \Psi_{j,k+1,l} + \Psi_{j,k-1,l} + \Psi_{j,k,l+1} + \Psi_{j,k,l-1} - 6\Psi_{j,k,l}). \quad (1)$$

The potential energy is given by the Coulomb potentials

$$V(r,t) = -\frac{1}{|\vec{r} - \vec{R}_{p1}|} - \frac{1}{|\vec{r} - \vec{R}_{p2}|} - \frac{Z_i}{|\vec{r} - \vec{R}_i|} \quad (2)$$

where $\vec{R}_{p1}$ is the position of proton 1 (and similar for 2), Z_i is the charge of the ion, and $\vec{R}_i$ is the position of the ion. To be specific, we will choose the z direction to be the direction of the ion velocity.

Unlike previous calculations for ion scattering, we have not used a soft-core potential. Instead, the positive charges are positioned to always be between grid points. The stationary charges are always situated so their positions are at the center of a cube whose corners are grid points; the position has the form $(x+[\Delta x/2], y+[\Delta x/2], z+[\Delta x/2])$ where (x,y,z) is the position of a grid point. The moving charge(s) will always have the velocity in the z direction and are positioned so that the (x,y) position is at the center of a square whose corners are grid points; the position has the form $(x+[\Delta x/2], y+[\Delta x/2], z)$ where (x,y) are positions of grid points. This prescription keeps the Coulomb singularities as far as possible from the grid points. Using this prescription, the energy of the eigenstates changes as the ion moves but the change is minimal.

As an example, when we choose $\Delta x = 1/7$ a.u., the energy of H_2^+ for an internuclear separation of 2 a.u. is -0.5993 a.u. when both protons are at the center of the cube defined by grid points and -0.6010 a.u. when both protons are at the center of a face of the cube; the exact value is -0.6026 a.u.When both protons are at the center of the cube, we found that the error in the calculated ground-state energy using the grid was 0.16 a.u. Δx^2 for $\Delta x = 1/5, 1/6, \ldots, 1/10$ a.u. Forcing the ions to be halfway between grid points also causes a small difficulty when we want to have the H_2^+ oriented at angles other than 0° or 90°; namely, the grid spacing has small changes for different tilt angles. For example, for a tilt angle of 45° and an internuclear separation of 2 a.u., the two protons can be separated by 10 grid spacings in x and 10 grid spacings in z if the $\Delta x = 1/\sqrt{50}$ a.u. which is a slight change from the $\Delta x = 1/7$ a.u. used for 0° or 90°.

The initial electronic state and the excited states of H_2^+ are computed by a relaxation technique. Approximate eigenstates on the grid are generated from the analytic wave function in spheroidal coordinates [7]. We then iteratively solve for the eigenstate state n, using $\psi_n \rightarrow (E-H)\psi_n$ where E is roughly the maximum eigenenergy for H. This method is equivalent to a first-order approximation of the exponential relaxation method [multiply by $\exp(-H\tau)$ with $\tau = 1/E$]. To see how this method works, write the wave function in terms of the unknown eigenstates of H, ψ_j. After one multiplies by $E-H$, the state $\psi = \Sigma_j a_j \psi_j$ goes to $\psi = \Sigma_j (E-E_j) a_j \psi_j$. If E is chosen to be roughly the maximum eigenenergy of H, then $E-E_j$ is largest for the ground state even though we do not know a_j, E_j, or ψ_j. After renormalizing ψ the ground-state fraction of ψ increases. We repeatedly multiply by $E-H$ until the wave function remains unchanged to an acceptable tolerance. For the calculation of excited states this procedure would drive the state to the ground state so we orthogonalize the excited states to the lower-energy states after every iteration.

The discretized Schrödinger equation for the electron is solved using the staggered leapfrog algorithm [8]. This algorithm gives an explicit equation for the wave function propagated by a time step Δt. The staggered leapfrog algorithm exactly conserves the norm for a time-independent Hamiltonian when the time step is less than $1/E_{\max}$ where $E_{\max}$ is

the maximum energy of the Hamiltonian. For time-dependent Hamiltonians, the norm is only approximately conserved for this condition but the errors in the norm are small for the small Δt used in our propagation. A difficulty with this method is the steep increase in CPU time as Δx decreases. The number of operations is proportional to the number of mesh points which is proportional to Δx^{-3} and the time step decreases proportionally to Δx^2 to satisfy the propagation condition on the leapfrog algorithm. Thus, the CPU time is proportional to Δx^{-5}: decreasing Δx from 1/5 to 1/7 a.u. increases the CPU time by a factor of 5.4.

The electron is initially in the ground state of H_2^+, which depends on the positions of the protons. In our calculations of the excitation cross section, the protons of the H_2^+ are fixed in space and the ion has a velocity v_i. After the ion has passed the H_2^+, we project the wave function onto the electronic eigenstates of the H_2^+ molecular ion as calculated on our grid. For the excitation cross section, we used a grid spacing of $\Delta x = 1/5$ a.u. Our spatial grid of points covers the range $-19.2 \leqslant x, y \leqslant 19.2$ a.u. and $-25.6 \leqslant z \leqslant 25.6$ a.u. The probability for the excitation to occur is $P_n = |\langle \psi_n | \Psi(t_{\text{fin}}) \rangle|^2$ where ψ_n is the eigenstate for state n of the H_2^+ and $\Psi(t_{\text{fin}})$ is the time-propagated wave function at the final time.

Because the ion velocity is in the z direcion, its time-dependent position can be written as $\vec{R}_i = (x, y, z_0 + v_i t)$. The cross section for excitation to state n is then

$$\sigma_n = \int \int P_n(x,y)dx\,dy = \int \int P_n(b,\phi) b\,db\,d\phi \qquad (3)$$

where $(x,y) = b(\cos\phi, \sin\phi)$. The symmetry of the Hamiltonian and the initial state allows us to compute the total cross section using only a restricted range of x, y, or ϕ. If we sum the cross section to each degenerate pair of Λ states, then the excitation cross section is twice the integral over the range $y \geqslant 0$ or equivalently $0 \leqslant \phi \leqslant \pi$. If the internuclear axis is perpendicular to the ion velocity vector only the range $x \geqslant 0$ and $y \geqslant 0$ is needed. If the internuclear axis is parallel to the ion velocity vector, we need to perform the calculation only along the line $y = 0$ and $x \geqslant 0$.

The charge transfer cross section was computed by fixing the ion in space and having the H_2^+ move with a velocity $-v_i$ in the z direction. This change of frame was done for the convenience of calculating the projection onto the final state; in this frame, the charge transfer final states are stationary. The initial electronic wave function is found by the relaxation technique described above. Because the H_2^+ is moving we multiply the initial electronic wave function by the factor $\exp(-iv_i z)$. For this series of calculations, we use a region $-20 \leqslant x, y \leqslant 20$ and $-25 \leqslant z \leqslant 25$ a.u. and a grid spacing $\Delta x = 1/7$ a.u. The H_2^+ starts with the center at $z = 20$ a.u. and the atomic ion is at $z = 5$ a.u. The calculation stops when the H_2^+ reaches $z = -20$ a.u. Because the atomic ion and H_2^+ are somewhat close, we compute the initial state of the H_2^+ in the presence of the atomic ion. At the starting time, we want the electron on the molecular ion. For He^{2+} scattering, we projected out the ground state of He^+ during the relaxation to prevent the electron from unphysically starting on the atomic ion.

The charge transfer cross section is computed in a manner similar to the excitation cross section. At the final time, we project the total wave function onto the analytic atomic eigenstates and integrate the probabilities over the two-dimensional impact parameters. We used the analytic atomic eigenstates for the projections (instead of the eigenstates on the grid) because we used a smaller grid spacing and we are mostly interested in total cross sections. For a couple of geometries, we compared results from projections on analytic atomic wave functions to results from projections on atomic eigenstates on the grid and found the cross section to an n-manifold differed by less than 1%.

For calculations of charge transfer in H^+ scattering from H_2^+, the cross section for a grid of $\Delta x = 1/5$ gave a value that differed by less than 1% from that for a grid of $\Delta x = 1/7$. Since we expect the error to scale like Δx^2 for small Δx, this suggests our errors are less than 2% for H^+ scattering. The He^{2+} scattering should be less accurate because of the larger charge but we expect the error to be less than 5% for this case.

C. Radial distribution

In the experiments of Ref. [2], "the D_2^+ molecular ions were created in a Penning ion source." The distribution of vibrational states from this source is not well known. However, it seems likely that the molecule is ionized in a single scattering event and the vibrational distribution can be approximated from the Franck-Condon overlaps. Unless the molecules were substantially heated above room temperature, the D_2 were all in the vibrational ground state [9]. We write the vibrational eigenstate of the molecule as $\chi_v(R)$ and for the molecular ion as $\chi_v^{(+)}(R)$.

The time from when the electron ionizes the D_2 molecule to the time the atomic ion passes is completely random on the time scale of the D_2^+ molecular ion. Thus, the phases of the different vibrational states will be random at the time of the atomic ion collision. When the phases of the vibrational states are random, then the radial distribution of the D_2^+ is the probability for being in a vibrational state times the square of the vibrational wave function summed over all vibrational states. The radial distribution of the ion is approximately

$$P(R) = \sum_v |\langle \chi_0 | \chi_v^{(+)} \rangle|^2 |\chi_v^{(+)}(R)|^2. \qquad (4)$$

The radial distributions for both H_2^+ and D_2^+ are shown in Fig. 1. The distribution extends to large R because the potential energy curves of the molecule and the positive ion are substantially shifted. The minimum for the neutral molecule is near 1.4 a.u. whereas for the ion it is near 2.0 a.u. This figure clearly demonstrates that large internuclear separations could be important when the ion is formed from a Franck-Condon-like process.

When a charge transfer occurs, the protons of the molecular ion have relatively little energy. The final kinetic energy of these protons will be mainly determined by the Coulomb repulsion. Because the internuclear separation correlates with the (measurable) kinetic energy of the protons, it should be

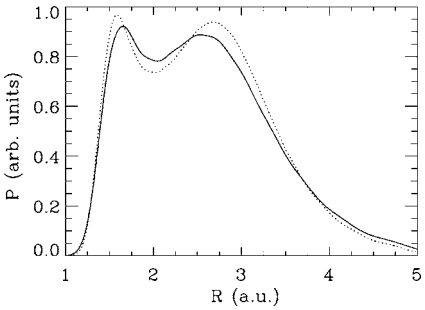

FIG. 1. The probability P for finding the internuclear separation at position R for H_2^+ (solid line) and D_2^+ (dotted line) if the molecular ion has a vibrational distribution given by the Franck-Condon overlaps with the neutral, vibrational ground state.

possible to experimentally determine how the cross section depends on internuclear spacing.

III. RESULTS

In this section, we describe the results of our calculations of excitation and charge transfer for collisions of H^+ and He^{2+} with H_2^+. For our approximations, the results are the same for H_2^+ and D_2^+. The emphasis is on the angular dependence of these processes. We present detailed results for ion velocities of 0.4, 0.5, and 1.0 a.u. as well as more general features over a larger velocity range.

A. He^{2+}

In Fig. 2 we show the angular dependence of the total charge transfer cross section as a function of the angle θ

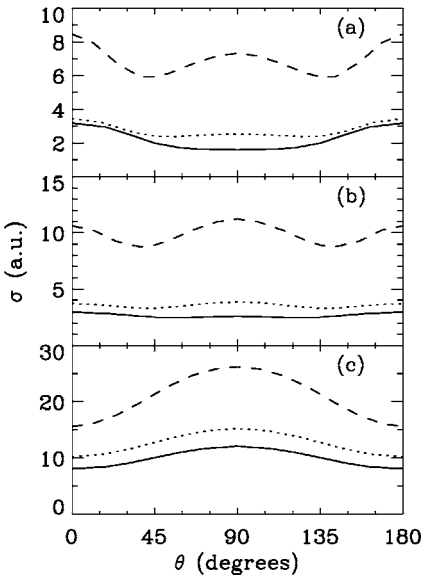

FIG. 2. The total charge transfer cross section as a function of the angle θ between the internuclear axis and the velocity vector of the He^{2+}. The three curves are for different internuclear separation: the solid line is 12/7 a.u., the dotted line is 14/7 a.u. (the minimum of the molecular ion potential), and the dashed line is 20/7 a.u. (a) is for an atomic ion velocity of 0.4 a.u., (b) is for 0.5 a.u., and (c) is for 1.0 a.u.

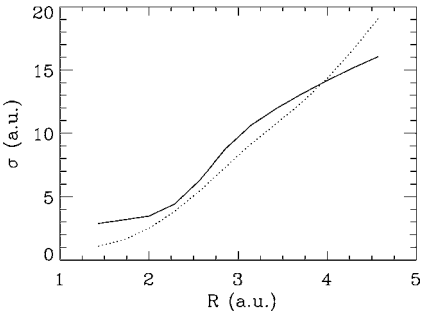

FIG. 3. The total charge transfer cross section as a function of the internuclear separation when He^{2+} has a speed of 0.4 a.u. The solid line is when $\theta=0°$ and the dotted line is for 90°.

between the internuclear axis and the velocity vector of the atomic ion. The three curves are for different internuclear separation: the solid line is 12/7 a.u., the dotted line is 14/7 a.u. (the minimum of the molecular ion potential), and the dashed line is 20/7 a.u. Figure 2(a) is for an atomic ion velocity of 0.4 a.u., Fig. 2(b) is for 0.5 a.u., and Fig. 2(c) is for 1.0 a.u. There are a couple of obvious trends in this figure. The cross section increases with increasing velocity over this region. Also, the cross section increases with increasing internuclear separation over this range. Most importantly, the cross section versus θ is relatively flat or is smaller at 90° than at 0° for velocities of 0.4 and 0.5 a.u. This behavior does not agree with the measurements of Ref. [2]. In their Fig. 6, the cross section at 90° is roughly four times larger than that at 0° at velocity of 0.4 a.u. and is roughly five times larger at velocity of 0.5 a.u. Our results are in qualitative agreement with the calculations of Ref. [5].

We can compare the angle-averaged charge transfer cross section to the results published in Refs. [1,4]. The peak of the charge transfer cross section is for a velocity of approximately 1 a.u. At an internuclear separation of 2 a.u., we have an angle-averaged cross section of approximately 14 a.u. which is somewhat larger than the calculation of Ref. [4] Fig. 4 of roughly 12 a.u. When we average over the distribution of R from the Franck-Condon overlaps, the cross section is substantially larger. We find the total charge transfer cross section is approximately 20 a.u. which is close to the measured and calculated cross section of Ref. [1] Fig. 2, approximately 21 a.u. However, the calculation of Ref. [4] is somewhat lower in Fig. 7, approximately 16 a.u. It is not uncommon for calculations and experiments to agree on total or averaged cross sections but to differ on partial or differential cross sections since these are more difficult to obtain for both experiment and theory, as in the present case.

From Fig. 1, we see that the D_2^+ could be at a large range of internuclear separation. Figure 3 shows the charge transfer cross section for a velocity of 0.4 a.u. for 0° and 90° over a range of internuclear separations. This figure clearly shows that at this velocity the cross section is of roughly equal size for the two angles over the range of likely internuclear separation. Another interesting feature is the increase of the cross section with internuclear separation which shows that the measurement emphasizes the large internuclear separation.

Figure 4 shows the cross section for the internuclear separation of 2 a.u. for 0° and 90° over a range of velocities.

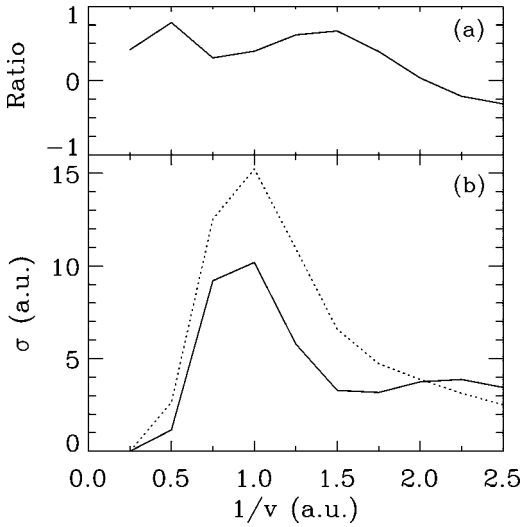

FIG. 4. The total charge transfer cross section as a function of the He^{2+} velocity when the internuclear separation is 2 a.u. (a) The ratio of the difference in cross section to the average cross section: ratio$=2(\sigma_{90}-\sigma_0)/(\sigma_{90}+\sigma_0)$. (b) The solid line is for $\theta=0°$ and the dotted line is for 90°.

Figure 4(b) shows the cross sections while Fig. 4(a) shows the ratio $2(\sigma_{90}-\sigma_0)/(\sigma_{90}+\sigma_0)$. We have plotted versus $1/v$ to emphasize features due to interference effects. The trend is for the cross section to be more peaked at 90° at higher velocities. However, there does appear to be an oscillation superimposed on this trend.

B. H^+

We performed the same calculations for H^+ as for the He^{2+} scattering. Figure 5 shows the total charge transfer cross section as a function of angle between the internuclear axis and the atomic ion velocity vector. The three curves in each figure are for the same separations as in Fig. 2: the solid

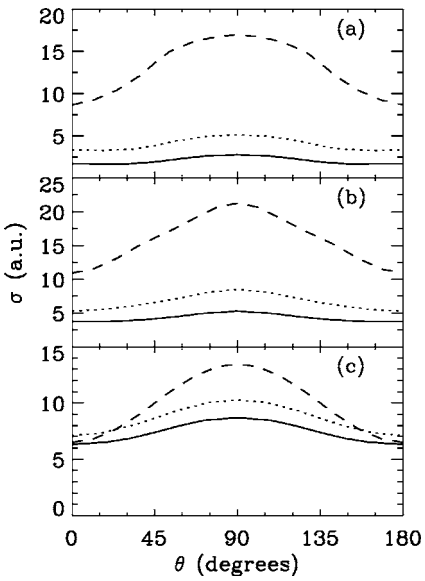

FIG. 5. Same as Fig. 2 but for H^+.

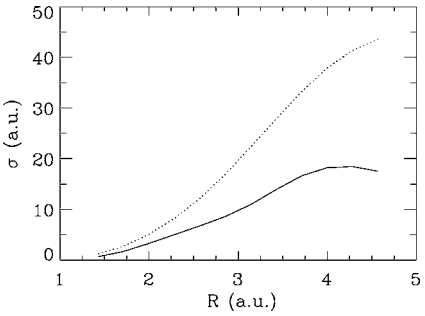

FIG. 6. Same as Fig. 3 but for H^+.

line is 12/7 a.u., the dotted line is 14/7 a.u. (the minimum of the molecular ion potential), and the dashed line is 20/7 a.u. The atomic ion velocities are also the same as in Fig. 2: Fig. 5(a) is for an atomic ion velocity of 0.4, Fig. 5(b) is for 0.5, and Fig. 5(c) is for 1.0 a.u. As with charge transfer to He^{2+}, the charge transfer cross section increases with velocity over this range. Also, the total charge transfer cross section increases with internuclear separation although not as rapidly as for He^{2+}. The main difference between He^{2+} and H^+ is for the lower velocities and near equilibrium internuclear separations: the charge transfer cross section is peaked at 90° for H^+ but at 0° for He^{2+}.

Figure 6 shows the dependence of the charge transfer cross section on the internuclear separation for an atomic ion velocity of 0.4 a.u. and orientations of 0° and 90°. Unlike the He^{2+} case, the angular dependence of the cross section increases with increasing separation so that the cross section is is strongly peaked at 90° at large R. When the H_2^+ ion is created with a range of internuclear separations, the increase of the cross section with R will cause the measurements to emphasize the large R angular dependence.

Figure 7 shows the cross section for the internuclear separation of 2 for 0° and 90° over a range of velocities. Figure 7(b) shows the cross sections while Fig. 7(a) shows the ratio $2(\sigma_{90}-\sigma_0)/(\sigma_{90}+\sigma_0)$. Unlike the results for He^{2+}, the ratio is larger than 0 for the whole range plotted and is typically

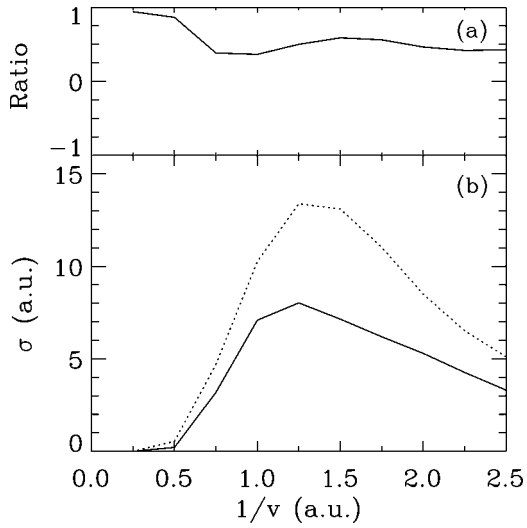

FIG. 7. Same as Fig. 4 but for H^+.

TABLE I. Partial charge transfer cross section in a.u. for He^{2+} at $R=2$ a.u.

	n for 0°			n for 90°		
v	1	2	3	1	2	3
0.4	0.03	3.25	0.16	0.03	2.41	0.07
0.5	0.15	3.27	0.33	0.15	3.62	0.11
1.0	0.70	8.71	0.78	2.25	12.0	0.97

TABLE II. Partial charge transfer cross section in a.u. for H^+ at $R=2$ a.u.

	n for 0°			n for 90°		
v	1	2	3	1	2	3
0.4	3.22	0.06	0.03	5.06	0.02	0.03
0.5	5.09	0.15	0.06	8.42	0.06	0.03
1.0	6.31	0.61	0.17	9.67	0.45	0.14

closer to 1, indicating the relatively stronger capture at $\theta=90°$. As in Fig. 4, the ratio shows a small but definite oscillation with velocity and at roughly the same velocities.

C. Tabulated data

In Table I, we give the charge transfer cross sections into specific n-manifolds for He^{2+} at $\theta=0°$ and 90°, and in Table II we give the results for H^+. These tables clearly show that the charge capture is mainly into one n-manifold at the lower velocities. For the lower velocities, over 85% of the cross section is into the $n=2$ manifold for capture by He^{2+} while over 95% of the cross section is into the $n=1$ manifold for capture by H^+. Reference [1] found that charge transfer for He^{2+} was mostly into the $n=2$ manifold.

For the collisions with H^+, we also computed the excitation cross section into the low-lying excited states of H_2^+ for the equilibrium separation $R=2$ a.u. and the velocity of 0.5 a.u. The states of H_2^+ can be designated by the electron's angular momentum along the internuclear axis ($\Lambda=0$ is Σ, $\Lambda=\pm1$ is Π, etc.) and the reflection symmetry through the midpoint of the molecule along the internuclear axis (g is symmetric and u is antisymmetric). The excitation cross section is much larger when the velocity of the atomic ion is parallel to the internuclear axis. The excitation cross section into the lowest excited state with $^2\Sigma_u$ character is the largest cross section for both $\theta=0°$ and 90°: 6.54 a.u. for 0° and 0.57 a.u. for 90°; the $^2\Sigma_u$ state adiabatically connects to H^+ and H in $n=1$ at large internuclear separations. The cross section for excitation into the lowest-energy $^2\Pi_g$ state (we summed the contributions to the $\Lambda=1$ and -1 states) is next largest with 0.96 a.u. for 0° and 0.16 a.u. for 90°. The excitation cross section into the lowest excited $^2\Sigma_g$ state was smaller still: 0.15 a.u. for 0° and 0.03 a.u. for 90°.

IV. SUMMARY

We have calculated the charge transfer and excitation cross sections for H^+ and He^{2+} collisions with H_2^+ molecular ions. The calculations focus on the orientation dependence of these processes which is quite strong. Our results for the dependence of the charge transfer on the angle between the internuclear axis and the ion velocity vector disagree with the measurements and calculations of Ref. [2] for He^{2+} projectiles but agree with the calculations of Ref. [5]. The measurements are in clear disagreement with the present calculations but it is unclear where the problem resides. The current calculations have almost no approximation except the apparently very accurate ones associated with treating the heavy particles classically and associated with computing the wave function on a grid of points. Since this is the simplest example of ion-molecule collision, it is perhaps worthwhile for other researchers to undertake this problem with different methods. Our angle-averaged charge transfer cross sections agree with the measurements and calculations of Ref. [1].

In addition to this, we found the cross section strongly increases with internuclear separation; the increase is sufficiently strong that the measurements mostly sample large internuclear separation. We have found that the cross section as a function of the angle between the velocity of the incoming ion and the axis of the H_2^+ molecular ion strongly depends on the speed of the incoming ion. We have plotted $2(\sigma_{90}-\sigma_0)/(\sigma_{90}+\sigma_0)$ versus $1/v$ and found an oscillation superimposed on the general trend. We find the excitation cross section by H^+ at $v=0.5$ a.u. to strongly depend on the orientation and is dominated by excitation into the lowest $^2\Sigma_u$ state at the equilibrium separation.

ACKNOWLEDGMENTS

We gratefully acknowledge extended conversations with B. D. Esry. D.J.P. was supported by the NSF "Research Experience for Undergraduates" program. This work was supported by the Chemical Sciences, Geosciences, and Biosciences Division of the Office of Basic Energy Sciences, U.S. Department of Energy. Computational work was carried out at the National Energy Research Scientific Computing Center in Oakland, CA and the Center for Computational Sciences at the Oak Ridge National Laboratory, TN.

[1] H. Bräuning, I. Reiser, A. Diehl, A. Theiß, C. L. Cocke, and E. Salzborn, J. Phys. B **34**, L321 (2001).
[2] I. Reiser, C. L. Cocke, and H. Bräuning, Phys. Rev. A **67**, 062718 (2003).
[3] R. Shingal and C. D. Lin, Phys. Rev. A **40**, 1302 (1989).
[4] J. Caillat, A. Dubois, I. Sundvor, and J.-P. Hansen, Phys. Rev. A **70**, 032715 (2004).
[5] S. C. Cheng and B. D. Esry, Phys. Rev. A **72**, 022704 (2005).
[6] A. Kolakowska, M. S. Pindzola, F. Robicheaux, D. R. Schultz, and J. C. Wells, Phys. Rev. A **58**, 2872 (1998).
[7] D. R. Bates, K. Ledsham, and A. L. Stewart, Philos. Trans. R. Soc. London, Ser. A **246**, 215 (1953).
[8] W. H. Press, S. A. Teukolsky, W. T. Vetterling, and B. P. Flannery, *Numerical Recipes* (Cambridge University Press, New York, 1992).
[9] The first vibrational state of D_2 is approximately 3000 cm^{-1} (roughly 4300 K) above the ground state.